Carbon dioxide, methane and nitrous oxide fluxes from a fire chronosequence in subarctic boreal forests of Canada

Koster, Egle

2017-12-01

Koster , E , Koster , K , Berninger , F , Aaltonen , H , Zhou , X & Pumpanen , J 2017 , '
Carbon dioxide, methane and nitrous oxide fluxes from a fire chronosequence in subarctic
boreal forests of Canada ' , The Science of the Total Environment , vol. 601 , pp. 895-905 . https://doi.org/10.1016/j.s

http://hdl.handle.net/10138/310370
https://doi.org/10.1016/j.scitotenv.2017.05.246

*Graphical Abstract

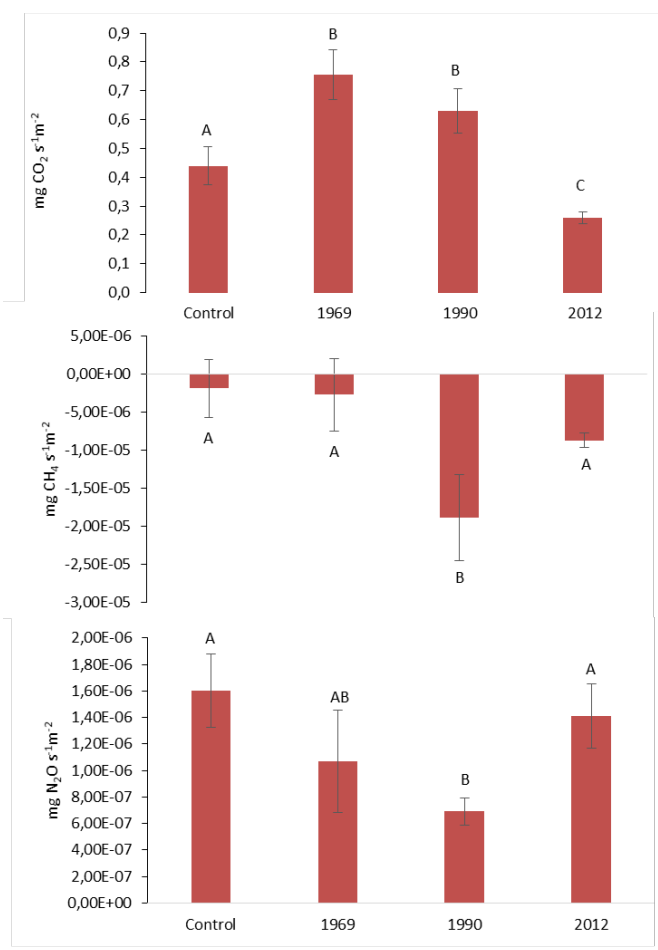

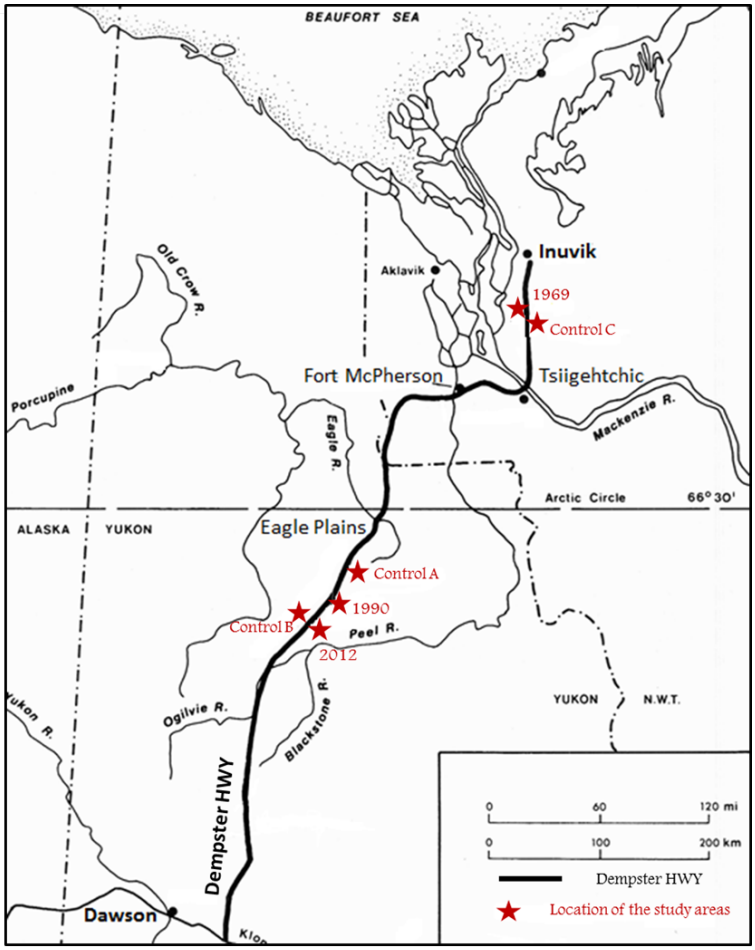

Highlights

- An increase in the active layer thickness results in higher GHG emissions.
- A fire chronosequence study reveals long-term changes in GHG emissions.
- The only factor affecting studied GHG fluxes is the time since last forest fire.
- Fire causes long-lasting changes of GHG emissions.

Carbon dioxide, methane and nitrous oxide fluxes from a fire chronosequence in subarctic boreal forests of Canada.

Egle Köster[1,*], Kajar Köster[1,2], Frank Berninger[1], Heidi Aaltonen[1], Xuan Zhou[1], Jukka Pumpanen[3]

[1] Department of Forest Sciences, University of Helsinki, P.O. Box 27, FI-00014 Helsinki, Finland

[2] Department of Biosciences, Viikki Plant Science Centre, University of Helsinki, FI-00014 Helsinki, Finland

[3] Department of Environmental and Biological Sciences, University of Eastern Finland, PL 1627, FI-70211 Kuopio, Finland

[*] Corresponding author:

Egle Köster, PhD

University of Helsinki

Department of Forest Sciences

P.O. Box 27, FI-00014 Helsinki

Tel: +358400258370

e-mail: egle.koster@helsinki.fi

Field Code Changed

Abstract

Forest fires are one of the most important natural disturbances in boreal forests, and their occurrence and severity are expected to increase as a result of climate warming. A combination of factors induced by fire leads to a thawing of the near-surface permafrost layer in subarctic boreal forest. Earlier studies reported that an increase in the active layer thickness results in higher carbon dioxide (CO_2) and methane (CH_4) emissions. We studied changes in CO_2, CH_4 and nitrous oxide (N_2O) fluxes in this study, and the significance of several environmental factors that influence the greenhouse gas (GHG) fluxes at three forest sites that last had fires in 2012, 1990 and 1969, and we compared these to a control area that had no fire for at least 100 years. The soils in our study acted as sources of CO_2 and N_2O and sinks for CH_4. The elapsed time since the last forest fire was the only factor that significantly influenced all studied GHG fluxes. Soil temperature affected the uptake of CH_4, and the N_2O fluxes were significantly influenced by nitrogen and carbon content of the soil, and by the active layer depth. Results of our study confirm that the impacts of a forest fire on GHGs last for a rather long period of time in boreal forests, and are influenced by the fire induced changes in the ecosystem.

Keywords: permafrost, greenhouse gas, forest fire, active layer, GHG flux

1. Introduction

Approximately 35% of the world's forest area is covered by northern boreal forests that grow in Canada, Alaska, Russia and Northern Europe (Kim and Tanaka, 2003). These forests have an important role in global carbon (C) balance as they contain about 66% of the world's forest soil

carbon pools (Kasischke and Stocks, 2000), and even small changes in these pools have a significant impact on the greenhouse gas (GHG) balance of the atmosphere. Generally boreal ecosystems are C sinks that absorb atmospheric carbon dioxide (CO_2) releasing it slowly from decomposing organic matter (Fan et al., 1998). The presence of permafrost makes these high latitude ecosystems especially vulnerable to changing climate (Kim and Tanaka, 2003). Increases in the depth of the seasonally thawed active layer may increase soil temperature, and with it the rate of decomposition (Grosse et al., 2011). Increased depth of active layer might also decrease soil moisture, which would also increase the rate of decomposition (Zona, 2016).

Climate warming results in the increase in occurrence of forest fires, which act as one of the predominant natural disturbances in boreal forests (Stocks et al., 1998; Kim and Tanaka, 2003). It is estimated that around 5-15 million hectares of forests burn annually in the boreal biome (Stocks et al., 1998; Kasischke and Stocks, 2000; Conard et al., 2002). The trend of annual fire events in Canada has increased steadily from approximately 6000 in 1930-1960 period to 9000 fires in 1980s and 1990s period (IFFN, 2004). A retrospective analysis of C fluxes have found that since 1980 Canadian forests have been a net source of atmospheric C primarily due to increasing fire regimes, which is indirectly related to climate change, land use changes and fire suppression (Kurz and Apps, 1999; Houghton et al. 2012). Fire is an extremely important factor in the dynamics of Canadian forests, since some of the most important species require event of a fire for regeneration to occur (Sirois, 1993). The occurrence of forest fires also determines the successional pathways in boreal areas (Gewehr et al., 2014). Severe fires have been found to accelerate the degradation of permafrost (Burn, 1998; Taş et al., 2014), and further succession of the areas is likely to be modified by permafrost decline. Thus, the increase of fire severity, and shorter fire return intervals in the Canadian forests during the last 50 years (IFFN, 2004), has led to an increase in the distribution of younger stands and a decrease in the C storage (Stocks et al.,

66 1998; van Bellen et al. 2010). Furthermore, different studies suggest that the severity of forest
67 fires and the overall burned area is going to increase near the end of the 21st century as the
68 weather will be drier and the fire season peak is going to shift towards the end of the summer
69 (Flannigan et al., 2000; van Bellen et al., 2010).

70 Forest fires strongly influence soil C dynamics (Amiro et al., 2009; Dore et al., 2008; Sullivan et al.,
71 2011). A pulse of CO_2 and other GHGs is released into the atmosphere as an immediate effect of
72 the fire (Nakano, 2006; Sullivan et al., 2011). It has also been found that soil GHG fluxes that
73 originate from the decomposition and respiration processes are affected for a long period of time
74 after the fire episode (Hart et al., 2005; Cairney and Basitas, 2007; Köster et al., 2015). Permafrost
75 areas are also strongly influenced by fire as combustion removes the insulating organic layer. This
76 in turn causes a decrease in surface albedo and increases the soil thermal conductivity from about
77 fivefold to tenfold (Hinzman et al., 1991; Yoshikawa et al., 2003). Consequently, numerous studies
78 have well documented the phenomenon that fire evoked changes in the permafrost and thickness
79 of the active layer. Several of these studies concern the effects of fire in natural conditions
80 (Kryuchkov, 1968; Viereck, 1982; Brown, 1983; Yoshikawa et al., 2003), but studies from controlled
81 field experiments are also available (Dyrness, 1982). Results indicate that heat from the fire itself
82 does not significantly affect the active layer (Dyrness, 1982; Viereck, 1982; Brown, 1983;
83 Yoshikawa et al., 2003). However, the depth of the active layer increases after the forest fire for
84 approximately 3–5 years, depending on the severity of fire and site conditions (Dyrness, 1982;
85 Viereck, 1982; Brown, 1983; Yoshikawa et al., 2003) due to changes in ground vegetation coverage
86 and albedo, resulting in higher ground temperatures after disturbance (Tsuyuzaki et al., 2008).
87 These changes directly influence the emissions of CO_2 and other GHGs into the atmosphere
88 (Kasischke et al., 1995; Kim and Tanaka, 2003; Suk, 2013).

89 Forest fires directly influence ecosystem C dynamics by reducing the total C storage and increasing
90 the proportion of necromass in ecosystem C pools (Amiro et al., 2009; Dore et al., 2008; Sullivan et
91 al., 2011). The decomposition such a necromass typically releases about three times more CO_2
92 from the soil than the direct emission from the burning event (Auclair and Carter, 1993; Burke et
93 al., 1997). This post-fire CO_2 release seems to be strongly dependent on soil moisture conditions
94 and temperature (Ullah and Moore, 2011).

95 Fluxes of another C based GHG, methane (CH_4), are also influenced by fire. Non-paludified boreal
96 forest are usually sinks of CH_4 (Kulmala et al., 2014; Köster et al., 2015). Some researches show
97 that after a fire the uptake of CH_4 increases, returning to initial unburned conditions after one year
98 in a southern boreal forest (Kulmala et al., 2014; Taş et al., 2014). It is suggested that the main
99 reason for this is the fast recovery of the microbial community in the soils (Hamman et al., 2007;
100 Kulmala et al., 2014). The fluxes of CH_4 are controlled by soil moisture and temperature, by the
101 time passed after the fire event, and by the availability of organic C (Poth et al., 1995; Nakano,
102 2006; Sullivan et al., 2011).

103 The third important GHG, nitrous oxide (N_2O), is produced by both aerobic (nitrification) and
104 anaerobic (denitrification) processes (Megonigal et al., 2004; Oertel et al., 2016). The emission of
105 N_2O is predicted to increase after the fire, as the post fire regrowth of vegetation increases the
106 amount of NH_4 (the basis for the nitrification processes) in the soil (Levine et al., 1988; Kim and
107 Tanaka, 2003). Studies have revealed that the changes in N_2O fluxes are hard to predict (Poth et
108 al., 1995; Anderson et al., 2013; Pihlatie et al., 2007; Köster et al., 2015), however they are
109 influenced by several soil physical, chemical and biological factors (Megonigal et al., 2004;
110 Butterbach-Bahl et al., 2013; Lenhart et al., 2015).

111 Although the effect of fire on permafrost forest areas has evoked the interest of scientists for a
112 rather long time (Kryuchkov, 1968; Hinzman et al., 1991; Yoshikawa et al., 2003; Tsuyuzaki et al.,
113 2008), the changes in the uptake and emissions of different GHGs caused by forest fire have
114 received less attention (Kasischke and Stocks, 2000; Kim and Tanaka, 2003). The main topic of the
115 earlier research in most cases, was C and its balance in the ecosystem (Kurz and Apps, 1999;
116 Kasischke et al., 1995; Kasischke and Stocks, 2000), and few studies also observed the influences
117 of fire on GHGs during a short period of time that had elapsed after the forest fire (Kim and
118 Tanaka, 2003; Takakai et al., 2008). However, according to our knowledge, there are no studies
119 made on long-term effects of fire on three main GHG (CO_2, CH_4 and N_2O) fluxes in permafrost
120 areas. As stated above, the GHG fluxes resulting from the decomposition of necromass are much
121 larger than the instantaneous GHG emissions released in fire. Also, the recovery of the ecosystem
122 C pools takes several decades (Köster et al., 2014). We investigated in this study a longer-term
123 chronosequence of forest fires in boreal coniferous forests that have permafrost base in the north-
124 western part of Canada. Areas that had differing time periods since the last forest fire, but which
125 had comparable ecological conditions, were chosen for testing the long term impact of fire on CO_2,
126 CH_4 and N_2O fluxes. We compared the significance of experimental factors that act over time since
127 the fire event, the measurement time, soil moisture, depth of active the layer, tree biomass and
128 ground vegetation biomass, and soil temperature that influence the GHG fluxes across a fire
129 chronosequence. Our key research question was: how does the time that has elapsed since the
130 last fire influence the CO_2, CH_4 and N_2O fluxes from soil in permafrost areas of a boreal forest. Our
131 hypotheses were that a) the fluxes of CO_2, CH_4 and N_2O will change as a consequence of fire and
132 the magnitude of changes correlates with the time since the last fire, b) the effects of fire will be
133 larger for carbon-based gases CO_2 and CH_4 than for N_2O due to low reactive N availability and
134 initially low N_2O fluxes in the boreal permafrost forest soils, and c) the fluxes of CO_2, CH_4 and N_2O

are positively correlated with the depth of the active layer above the permafrost during the vegetation period.

2. Material and methods

2.1. Study area

Our study areas were located along the Dempster Highway (total length of the highway 741 km), close to Eagle Plains (Yukon) (66°22' N, 136°43' W) and Tsiigehtchic (NWT) (67°26' N, 133°45' W) Canada (between the 280th and 670th kilometer points on the highway) (Fig. 1).

The altitude of the terrain in the region ranges from 150 to 600 m above the sea level and the bedrock is composed of a Cretaceous sandstone that is overlain by ice-rich moraine, glaciolacustrine silt and clay deposits and is underlain by continuous permafrost (Hadlari, 2006). The climate in the area is characterized by long cold winters with mean air temperatures well below 0°C from October till April. The mean annual air temperature in the area is -8.8°C, and the mean total precipitation is 248 mm (Environment Canada, 2009). The ecosystem of our study areas is taiga dominated by evergreen needle-leaved trees, *Picea mariana* (Mill.) BSP and *Picea glauca* (Moench) Voss. The ground vegetation is dominated by mosses and lichen species such as *Sphagnum* sp., *Cladonia* sp., Cladina sp., in addition to *Ericaceous* dwarf shrubs as *Vaccinium vitis-ideaa* L.*, Rhododendron groenlandicum* Oeder.*, Rubus chamaemorus* L.*, Vaccinium uliginosum* L. and typical minor taiga plant species (Meikle and Waterreus, 2008).

Field Code Changed

Soils in the study areas are classified into the Cryosolic Order according to the World reference base for soil resources (IUSS Working Group WRB, 2015). These are described as soils of the arctic and tundra regions; soil-forming processes are dominated by the presence of permafrost (Stanek,

1982; Kimble, 2004). A cryic horizon starting ≤ 100 cm beneath the soil surface and diagnostic horizons are affected by cryoturbation, which is the soil movement that arises from frost action. The soils in the areas are predominately slightly acidic (Stanek, 1982, IUSS Working Group WRB, 2015).

2.2. Study design

In the summer of 2015, four different study areas, each with a different time since the last stand replacing forest fire (age class), were established thus: areas with last forest fire in 2012, 1990 and 1969, and fourth area was a control which had no fire for at least 100 years (Fig. 2). The dates of the fires were determined from the Yukon and Northwest territories fire maps. A hierarchical sampling procedure was adapted in the four study areas. At each age class area we established three 150 meter-long-lines with three sample plots along each line at 50 meter intervals. The lines were spaced by at least a few hundred meters from each other. We thus had nine sample plots per age class. The study lines were placed in the areas so that they were at least 150 m from the nearest road to avoid the disturbance of the road on the snow cover and consequently on permafrost (Gill et al., 2014). In addition, the lines were placed in as flat topography of terrain as possible to minimize the effect of the topographic variation. The measurements of stand characteristics were performed on three sample plots (400 m^2) as follows: ground vegetation cover, biomass and species composition, tree biomasses and tree densities were measured and then the mean values for each of these characteristics were calculated. Ground vegetation biomass was measured at four 0.20 x 0.20 m squares per sample plot. Specific composition of ground vegetation and coverages of each species were estimated visually from entire sample plot and coverages (%) of vascular plants, lichens and mosses were estimated at 0.75 x 0.75 m squares.

Characteristics of all trees (starting with 1 m height) inside the sample plots were measured (stem diameter at 1.3 m height, the height of a tree, crown height and crown diameter). The diameter for trees lower than 1.3 m was measured close to the ground. The formulas of Lambert et al. (2005) were used for tree biomass calculations. The tree biomass for the area burned in 1990 was calculated separately assuming 1.30 m seedling height and using an equation for spruce (Wagner and Ter-Mikaelian, 1999).

The soil texture on our study areas was very fine-silty clay loam, and the control area had the finest texture of silt loam. The soil moisture content was rather high during the whole measurement period (37.2–54.9 %) (Table 1). One soil pit was excavated in the middle of each sample plot (nine replicates per age class). Soil samples were taken from the litter and humus layer, and if possible, from the mineral soil at 0.05 m, 0.10 m, 0.30 m and 0.50 m depths and as close to the permafrost as possible, from three different walls of the soil pit. We used a steel corer (0.06 m diameter, 0.06 m in length) for collecting of soil samples from the vertical face of the soil pit for measuring basic soil profile properties such as soil C and nitrogen (N) contents, pH, texture and for determining the temperature sensitivity of soil respiration (Q10) with soil incubations in the laboratory. The depth of the active layer above the permafrost was also measured at each sample plot for calculating the mean depth of the active layer for all areas. When the permafrost could not be reached, the depth of the active layer was calculated using a linear extrapolation of the soil temperature profile for the mineral soil. The soil pH, soil C and N contents in the present study were measured in all collected samples at 0.05–0.50 m depths.

The soil samples used for soil incubations, soil C, soil N concentration and pH measurements were stored at 4°C, until analyses. Prior to the analyses, roots and stones were separated from the soil which was homogenized by sieving it through a 2 mm sieve. Soil pH was analysed using a glass

electrode (Standard pH meter, Radiometer Analytical, Lyon, France) in 35 mL soil suspensions, consisting of 10 mL of the soil sample and 25 mL of ultrapure Milli-Q water (left overnight to stand after mixing). Soil dry weight was measured after incubation by drying the homogenized soil samples at 105°C for 24 h. The dried samples were further homogenized by grinding them with a mortar grinder (Retsch Type RMO, Bioblock Scientific, Haan, Germany) and the C and N concentrations were then measured using an elemental analyzer (varioMAX CN elemental analyzer, Elementar Analysensysteme GmbH, Germany).

2.3. Chamber measurements of CO_2, CH_4 and N_2O and soil incubation

The static chamber method was used for measurements of CO_2, CH_4 and for N_2O fluxes between the soil and the atmosphere (Pumpanen et al., 2004; Pihlatie et al., 2013). Gas flux measurements were taken during the summer of 2015 from metal collars (on 18 collars per fire age class with diameter 0.21 m and height 0.05 m) that had been placed into the soil before measurements. The lower edge of the collar was placed at 0.02 m depth in the mor layer above the rooting zone to avoid damaging the roots. All chamber measurements were carried out during the daylight. The vegetation inside the chamber was not damaged or removed during the measurements.

A cylindrical chamber (h=0.24 m and Ø=0.20 m) covered with aluminium foil (to prevent photosynthesis), was used in the flux measurements. Circulation of air inside the chamber was provided by a small fan (0.025 m in diameter). The CO_2 concentrations inside the chamber were measured using a non-dispersive infrared CO_2 probe (GMP343, Vaisala Oyj, Helsinki, Finland) and the relative humidity and temperature with RH-/T-sensor (HMP75, Vaisala Oyj, Helsinki, Finland) at 5 sec intervals for 4 min during the 5 min chamber deployment time. The first 30 sec after placing

the chamber onto the collar were discarded from the measurement data to exclude the disturbance effects of the chamber deployment.

The CH_4 and N_2O flux measurements were done separately from the CO_2 efflux measurements, but they were taken from the same collars and using the same chamber as in the CO_2 efflux measurements. The chamber was equipped with an outlet tube that could be closed and opened with a 3-way valve for the air sampling (BD Connecta TM Stopcock, Becton Dickinson, NJ, USA). The CH_4 and N_2O gas samples were collected from the chamber headspace by connecting a 50 ml polypropylene syringe (BD Plastipak 60, BOC Ohmeda, Helsingborg, Sweden) equipped with a similar 3-way valve to the outlet tube of the chamber. Air samples were collected before the chamber placement (0 min) and at 1, 5, 10 and 20 minutes after the chamber was placed on the collar and injected immediately into glass vials (12 ml Soda glass Labco Exetainer®, Labco Limited, UK) for storage and transportation. The samples were analysed by an Agilent Gas Chromatograph model 7890A (GC, Agilent Technologies, USA) equipped with an autosampler (Gilson GX-271 Liquid Handler) and fitted with a Flame Ionization Detector (FID). Helium (45 ml min^{-1}) was used as the carrier gas and synthetic air (450 ml min^{-1}) and hydrogen (40 ml min^{-1}) were used as the flame gases, and 5 ml min^{-1} of N_2 was used as the make-up gas for the FID. Oven temperature was 60°C, and the detector temperature was 300°C. Samples were analysed by plotting their concentration emission readouts against a six-point standard curve (Pihlatie et al., 2013). The linear regression fitted to time and concentration change inside the chamber headspace was used for calculations of CO_2, CH_4 and N_2O fluxes. Outliers from the CH_4 and N_2O concentrations were measured during each chamber deployment and were then subjected to filtering by using Grubbs' test for outliers (Grubbs, 1969; Stefansky, 1972). The filtering of the outliers was based on the deviation of individual data points from the slope of the linear regression line and the standard deviation of the data points along-side the regression line.

249 Soil temperature was measured at each chamber during the flux measurements at 0.1 m depth
250 with a digital thermometer. Soil water content measurements were taken using soil moisture
251 sensors (Thetaprobe ML2x, Delta-T Devices Ltd, Cambridge, UK) that had been connected to a data
252 reader (HH2 moisture meter, Delta-T Devices Ltd, Cambridge, UK)) at each chamber.

253 The temperature sensitivity of soil respiration was measured from the homogenized samples in
254 field moisture by incubating 25 ml of sample in glass bottles (500 ml in volume) at 1, 7, 13 and
255 19°C for 24 h. The bottles, and also the blanks without the soil, were first flushed with technical air
256 (AGA, Finland) and closed air tightly with rubber stoppers. After each 24 h incubation air samples
257 were taken from the headspace of the bottles by 50 ml polypropylene syringe (BD Plastipak 60,
258 BOC Ohmeda, Helsingborg, Sweden). The air samples were injected immediately into the glass
259 vials (12 ml Soda glass Labco Exetainer®, Labco Limited, UK). The CO_2 concentrations were
260 measured from the headspace samples as described above and the respiration rates were
261 calculated from the CO_2 concentration increases in the headspace samples over the 24 h
262 incubations. The respiration rates were used to determine the respiratory temperature coefficient,
263 Q_{10}.

264

265 2.4. Data analyses

266 The CO_2 effluxes between different age classes were compared and the CO_2 emissions measured
267 in the field were corrected for soil temperature, as soil surface CO_2 efflux has been shown to
268 display a nonlinear response to temperature (Rayment and Jarvis, 2000). Soil CO_2 efflux was
269 corrected assuming that respiration (*R*) is an exponential function of temperature.

270

$$R_{corr} = R\ Q_{10}^{(T-T_{ref})/10} \quad (1)$$

, where R_{corr} is the T corrected soil CO_2 efflux, Q_{10} is the respiratory temperature coefficient, T is the measured soil temperature and T_{ref} is the reference temperature where the CO_2 effluxes were corrected. In this case, the T_{ref} used was the mean soil temperature at 10 cm depth during all CO_2 efflux measurements.

A separate temperature sensitivity coefficient, Q_{10}, was calculated for every age class to prevent the differences induced by soil properties, vegetation and different measuring temperatures (Kätterer et al., 1998; Wang et al., 2006; Köster et al., 2014). The Q_{10} fitting was performed using Python programming software. The analysis and calculations for the temperature sensitivity coefficients (Q_{10}) of the different age classes were: 2012 = 2.98, 1990 = 2.61, 1960 = 2.94, control area = 2.60. The CH_4 and N_2O temperature sensitivity coefficient Q_{10} were not calculated. Data was checked for normality using the Shapiro-Wilk test and a logarithmic transformation was made for the recorded CO_2 fluxes. A Tukey's HSD post hoc test was used for comparison of age class effects for all measured GHG fluxes ($P < 0.05$ were considered to be significant differences).

Linear mixed effect model was used for explaining experimental factors affecting the GHG fluxes. Time since the fire (age class) (*Yr*), soil temperature at 0.1 m depth (*ST)*, moisture (*MOI*), active layer depth (*AD*), tree biomass (*TB*) and ground vegetation biomass (*GB*) and the interaction between soil temperature and active layer depths (*ST × AD*) were included as fixed effects in the initial model, whereas the collars in each sample line (*YL*) were treated as a random effect We selected the best model using stepwise selection. We started with a full model and reduced the

number of variables using the AIC as the selection criteria. This was done using the drop1 function (Chamers, 1992) in R. The time since the fire, as our experimental treatment was always retained in the model.

The initial model including all factors was:

$$GHG = a + b\,Yr + c\,ST + d\,MOI + e\,AD + f\,TB + g\,GB + h(ST \times AD) + rYL \qquad (2)$$

, where GHG is the greenhouse gas flux (non-temperature corrected CO_2, CH_4 and N_2O separately), *a* is the intercept of the model, *b*, *c*, *d*, *e*, *f*, *g* and *h* are the regression coefficients for the factors. The models' are presented in Table 2 with the AIC and adjusted pseudo r^2 values. The best model, with the lowest AIC and highest pseudo r^2 value. For each gas model, the normality model residuals were visually checked using quantile-quantile plot (Q-Q plot) (Faraway, 2002) method in R (RStudio, version 1.0.136, RStudio, Inc.). The linear mixed effect model analyses were carried out with R using "lme4" package (Bates et al., 2015).

3. Results

3.1. Fire impacts on soil properties and vegetation

Mean temperature in the area during July 2015 (when measurements were done), was 14.4°C and the mean monthly precipitation was 44 mm. The mean depth of the active layer on top of the permafrost in the areas ranged from 0.28 m in the control area to 1 m in the most recently burned areas (Table 1). The comparison of the areas showed that permafrost depths in the 2012, and 1990 areas were significantly different from the older burns ($P < 0.05$) whereas the difference between the control and the 1969 fire was not significant ($P = 0.054$). The recovery of the permafrost was observed, as in the area burnt in 1990 the active layer depth had already

314 decreased to 0.88 m and in the area burned in 1969 the active layer depth was 0.49 m (Table 1). A
315 negative correlation was observed between the time of the forest fire and soil temperature at 0.1
316 m depths (R = -0.503, P < 0.001) (Table 1). Mean soil temperature at 10 cm depth was the highest
317 in the more recently burned (forest fires in 1990 and in 2012) stands where it was found to be
318 around 7°C, i.e. about 3°C higher than in the control and in the 1969 burnt areas (Table 1). There
319 was a positive correlation between soil moisture, measured at 10 cm depth, and the time of the
320 forest fire (R = 0.334, P = 0.005) (Table 1). The lowest soil moisture was detected in the most
321 recently burned area, and the soil moisture was highest in the control area (Table 1). Soil pH
322 varied between 4.8–6.7, and was found to be lower in recently burned areas (R = -0.243, P =
323 0.045) (Table 1). The vegetation cover at our study areas was strongly affected by the time of the
324 last forest fire (Table 1, Fig. 2). The ground vegetation of the undisturbed control area was
325 characterized by full moss cover (*Sphagnum sp.* and *Pleurozium sp.*), covered by *Ledum*
326 *groenlandicum* Oeder,*Vaccinium vitis-idaea* L. and *V. uliginosum* L. shrubs and some *Rubus*
327 *chamaemorus* L. plants. The lichens of *Cladina sp.* were present in several plots. The ground
328 vegetation of the area burned in 1969 was rather similar to the control area, but there were fewer
329 lichens and more vascular plants present (*L. palustris*, *V. uliginosum* and *Betula nana* L.). The
330 *Dicranum* species could be found in addition to the *Pleurozium* in the mosses. The composition of
331 ground vegetation of the area burned in 1990 was mainly the same as described above, but there
332 were still some bare patches of soil present at that area. Several *Cladonia* species of lichens were
333 present in addition to *Cladina* species. The area burned in 2012 was characterized by many bare
334 patches of soil and obvious traces of burning on the ground, and there were still no living trees in
335 the area. The main species of vascular plants in the area was *Equisetum sylvaticum* L. (Fig. 2).

336

3.2. Fire impact on the fluxes of CO_2

We found that the temperature corrected CO_2 emissions in our study were significantly lower in the 2012 fire area) (Fig. 3). The CO_2 emissions increased throughout time period since the fire, and were highest for the area that had burned in 1969. The area burned in 2012 could be distinguished from all the others by having the lowest CO_2 emission (Fig. 3). The variation of CO_2 fluxes inside fire age classes (between the measured lines A, B and C) was found to be non-significant (Fig. 4).

When we used the mixed effect model analysis between CO_2 fluxes and experimental factors, we found that, of the variables measured, CO_2 emission was best predicted by the time since the fire (Table 2). The AIC and p–value indicated that the best model was model 7. The years after fire explained as much as 50% of the variation in CO_2 fluxes.

3.3. Fire impact on the fluxes of CH_4

Soil was found to be a sink for CH_4 in all the areas in our study. The CH_4 uptake was highest in the area burned in 1990. This was the only age class that had significantly different CH_4 fluxes compared with the others ($P < 0.001$). The uptake of CH_4 did not differ between the areas burned in 1969 and the control areas (Fig. 5). The flux of CH_4 showed a clear negative correlation with soil temperature (R = -0.384, P = 0.001) and positive correlation with soil moisture (R = 0.270, P = 0.026) and both soil moisture and soil temperature remained significant in the mixed model analysis.

The differences in CH_4 fluxes between the lines within the fire age classes were significant for areas burned in 1969 and in 1990 (P = 0.031 and P = 0.027, respectively). Although we observed the emission of CH_4 from control area and the area burned in 1969 on lines A, and lines B and C

359 acted as sink for CH_4, the differences in fluxes between the lines within the age classes were not
360 statistically significant (P = 0.161) (Fig. 6).

361 The best model for explaining the CH_4 fluxes (Table 2), indicated that the CH_4 flux was influenced
362 by the time passed since the last forest fire (P = 0.007), soil temperature (P = 0.017), active layer
363 depth (P = 0.011) and tree biomass (P > 0.05), whereas it was not affected by soil moisture and
364 ground vegetation biomass. During the model selection, we removed the ground vegetation
365 biomass from the original model to obtain the best model (Table 2, CH_4, model 2), and this model
366 explained 33% of the variation in CH_4 fluxes.

367

368 3.4. Fire impact on the fluxes of N_2O

369 Soil was a source of N_2O in all the studies areas. The N_2O emissions showed a slight decrease after
370 a forest fire, and were lowest in the area burned in 1990. This was also the only fire age class that
371 was significantly different from the others (Fig 7). The N_2O fluxes between the lines within each
372 age class were not significantly different from each other (Fig. 8).

373 The best model that explained the N_2O fluxes was Model 2, and it explained 30% of N_2O variation,
374 with lowest AIC and p-value. The model found no significant correlation between the N_2O flux and
375 the time passed since the last fire, whereas soil temperature (P < 0.001), active layer depth (P =
376 0.012) and the interaction of soil temperature and active layer depth (P = 0.002) were significantly
377 related to the N_2O emission.

378

379 4. Discussion

380 4.1. Fire impacts on soil properties and vegetation

We found that the depth of the organic layer strongly affected the permafrost depth, and the organic layer depths will increase over many decades or even centuries after a fire. We also showed in our study that forest fires, and in particular the time that had passed since the last fire event had substantial effects on the depth of the active layer that lies on top of the permafrost. Other studies have reported that the permafrost level reaches the pre-fire depth in 60 to 100 years (Viereck, 1983; Dyrness and Norum, 1983; Kasischke et al., 1995). There was a rapid increase in the active layer depth shortly after a forest fire in our study areas. The active layer extended to a one meter or more in depth in three years after the forest fire, but the permafrost recovered quite quickly over time (Table 1). A possible reason for this is the rather rapid recovery of ground vegetation in our study areas, which is one of the key factors for enabling the permafrost to recover to the pre-fire depth. Another important factor that was previously reported to increase the depth of the active layer is the combination of higher soil temperature and lower soil moisture (Kasischke et al., 1995).

We observed the highest soil temperatures in the area that had burned most recently (in 2012) and the lowest in the control area (Table 1), which can be explained by the change of soil top layer colour (due to the loss of vegetation cover reduction of humus layer and deposition of ash), and larger exposure to solar radiation (Viereck, 1982; Burn, 1998; Lyons et al., 2008; Pereira et al., 2013; Zavala et al., 2014). A number of studies about the effects of fire on the ground thermal regime have been published (Klock and Helvey, 1979; Liang et al., 1991; Yoshikawa et al., 2003; Takakai et al., 2008), but none of them studied the long-term effects of fire, unlike the present study. Nevertheless, all studies reported the soil temperature to increase shortly after the forest fire due to the combustion of protective vegetation and organic layer, and soil colour changes induced by ash cover (Sharrow and Wright, 1977, Yoshikawa et al., 2003; Sullivan et al., 2011; Köster et al., 2015). The vegetation is expected to re-establish over time, and this in turn will allow

405 the ground temperatures to cool down. Our results suggest that it takes about 50 years for sites to
406 re-gain their respective pre-fire thermal conditions.

407 Our results also found that the unburned control area had the highest soil moisture content,
408 whereas the driest soils in this study were at the areas burned in 2012 (Table 1). These findings are
409 similar to those observed by the working group chaired by Liang (1991) who also reported lower
410 soil moisture contents shortly after forest fire events in permafrost areas in China. Some studies
411 indicate that the soil moisture is expected to remain stable after the forest fire because decreased
412 plant transpiration compensates for the reduction of a protective plant canopy (Castaldi and
413 Fierro, 2005; Oertel et al., 2016). However another study has found that burnt and open areas
414 have lower rates of evapotranspiration compared to undisturbed areas (Kasurinen et al., 2014).
415 Yet other studies of permafrost areas have shown that the soil moisture content increases after
416 forest fires (Yoshikawa et al., 2003; Takakai et al., 2008). Both groups of authors reported that the
417 fires were followed by increase in soil moisture with the absence of vegetation (larch trees) and
418 reduced evapotranspiration (Yoshikawa et al. 2003; Takakai et al. 2008). Nevertheless, Takakai et
419 al. (2008) took their measurements in a rather wet year, and the Alaskan soils studied by
420 Yoshikawa et al. (2003) are known to be usually somewhat moist to wet. We suppose that the
421 lower soil moisture content observed in our study in the more recently burned areas can be
422 caused by the changed porosity of the top layer of the soil, as the soil moisture content was
423 measured at 10 cm depth. In addition the ground of more recently burned areas was darker
424 because of deposited ashes, and this in turn has caused the higher soil temperatures (Table 1). All
425 these factors in combination can be the reason of reduced soil moisture.

426 Soil pH of recently burned areas was found to be slightly lower than those of the areas with the
427 longer time intervals since the forest fire. We had expected to find the opposite, as the pH of fire

areas is strongly influenced by the alkaline ashes deposited on the ground (Pereira et al., 2013). It is possible that the pre-fire vegetation cover of recently burned areas was more characteristic to the paludal ecosystem, however it is hard to estimate as forest fires in the areas have been stand-replacing.

The vegetation cover in our study areas were strongly influenced by the forest fires, as all areas that had the fires also had stand replacement. We also noted a rather fast recovery at ground vegetation level in the areas where the fire had occurred in 1990, where the ground vegetation biomass and coverage were almost at the same level as those found in the control area. This indicates that succession of ground vegetation required only about 25 years to complete in our study areas.

4.2. Fire impact on the fluxes of CO_2

The effects of forest fires were not same for each GHG species investigated in our study. Soil CO_2 efflux was significantly decreased in the first years after the fire. The lowest CO_2 efflux was observed in the area burned in 2012, which was only three years before the measurements were taken and where the decrease after the forest fire was 53%. Our mixed effect model analysis indicated that the time since the fire event was the only factor that significantly distinguished the areas in case of CO_2 emissions. This result was expected and it could be partly caused by reduced root respiration in the absence of vegetation and changed soil pH (Kim, 2013; Oertel et al., 2016). Moreover, a substantial amount of SOM was combusted in the fire, and pyrogenic matter which is resistant to further decomposition, has been reported to form on the soil surface (Pereira et al., 2013; Knicker et al., 2017). A recent study observed that the immediate C losses from the burning of the forest floor corresponded to soil CO_2 effluxes for several years (Köster et al., 2014). Substantial changes were taking place in the proportion of autotrophic and heterotrophic

451 respiration in soil CO_2 efflux (Kulmala et al., 2014). We also observed that the surface soil C
452 storage decreased by 40% and soil CO_2 effluxes by 80% immediately after the fire. These changes
453 can be explained by alterations in the activities of fire affected extracellular enzymes in soil (Köster
454 et al., 2014, 2016). Similar results have been obtained in a series of studies, which reported a
455 reduction of 40–59% in CO_2 effluxes shortly after the forest fires (Kasischke and Stocks, 2000;
456 Richter et al., 2000; Sullivan et al., 2011). Many of these studies have stated that it takes no longer
457 than a decade, for CO_2 effluxes to recover after a forest fire (Burke et al., 1997; Kulmala et al.,
458 2014; Köster et al., 2015). We observed a clear increasing trend in CO_2 efflux over the 46 year
459 chronosequence after a forest fire, and the increase was the highest in the area burned in 1969
460 (Fig. 3). The CO_2 effluxes observed in the control area were smaller compared to those measured
461 in the area burned in 1969 and we suppose, therefore, that in permafrost areas the recovery of
462 CO_2 emission levels after the forest fire takes longer than generally assumed. We also suppose
463 that at the beginning of the recovery the CO_2 effluxes are correlated with the recovery of the
464 vegetation and the depth of the active layer. However the tree regeneration, that also affects CO_2
465 efflux, takes longer and this also has an effect on CO_2 efflux from the soil. Factors such as soil
466 temperature, soil moisture, C and N content of the soil can cause changes in CO_2 effluxes (Oertel
467 et al., 2016). Higher C and N content in the soil increases soil respiration (Oertel et al., 2016).
468 Although we had higher soil C and N concentrations in the control areas, we still observed lower
469 CO_2 effluxes when compared to the older areas. Saiz et al. (2006) have shown significantly higher
470 respiration rates at younger stands compared to more mature sites, but these sites were not
471 influenced by the fire.

472 4.3. Fire impact on the fluxes of CH_4

473 The soils in our study were mostly sinks for CH_4. Under aerobic conditions soils are predominantly
474 found to be CH_4 sinks (Fiedler et al., 2005; Oertel et al., 2016) as methanotropic microorganisms
475 are able to use CH_4 as a sole carbon and energy source (Megonigal et al., 2004). Therefore, CH_4 is
476 consumed rather than produced in dry arctic and boreal soils (Whalen et al., 1992; Hanson and
477 Hanson, 1996), whereas peatlands are mostly CH_4 sources. Some of the measurement plots in the
478 control area, and in the area burned in 1969, were found to be sources of CH_4 in the present
479 study. The emission of CH_4 from these plots was probably caused by the existence of peaty spots
480 within specific places within the plots of those two areas. This increase the variation in fluxes
481 within these two areas, but both areas were still predominantly found to be sinks of CH_4 as
482 indicated by their mean CH_4 fluxes. In addition to soil moisture content, fluxes of CH_4 have also
483 been found to be sensitive to soil temperature in conditions of lower temperatures, the processes
484 of methanogenesis decreases (Hanson and Hanson, 1996; Megonigal et al., 2004). The rather low
485 soil temperatures, which are characteristic of arctic and boreal soils are also a limiting factor for
486 the methanotrophic bacteria (Hanson and Hanson, 1996; Megonigal et al., 2004). We found
487 temperature to be a significant factor that influenced soil CH_4 fluxes and a positive correlation
488 could be observed between the soil temperature and increase in CH_4 uptake (Table 1, Fig. 5). We
489 observed a slight increase in the CH_4 uptake shortly after the fire (Fig. 5). The soil moisture was
490 also lower in the most recently burned areas (Table 1). This might result in smaller methanogenic
491 activity or higher methanotrophic activity leading to a small increase in methane uptake in the
492 recently burnt areas. Similar tendency has also been reported by several preceding studies (Burke
493 et al., 1997; Takakai et al., 2008; Sullivan et al., 2011; Kim, 2013; Kulmala et al., 2014; Köster et al.,
494 2015). The highest CH_4 uptake in most of these studies was observed shortly after the fire event
495 (Burke et al., 1997; Sullivan et al., 2011; Kulmala et al., 2014; Köster et al., 2015), whereas in our
496 current study the area that had burned 25 years prior to the measurements had significantly

497 higher CH_4 uptake compared to the others (Fig. 5). This can be accounted for the slightly higher
498 soil temperature measured in the area burned in 1990.

499 4.4. Fire impact on the fluxes of N_2O

500 All our study areas (age classes) acted as sources of N_2O, although some studies on GHG fluxes
501 reported boreal ecosystems to be a minor sink for N_2O (Pihlatie et al., 2007; Ullah and Moore,
502 2011; Köster et al., 2015). Our mixed effect model analysis revealed that the factors that influence
503 N_2O fluxes significantly were the N content of the soil, the C content of the soil, and also the depth
504 of the active layer. There are two main processes involved in N_2O production: denitrification under
505 anaerobic conditions, and nitrification under aerobic conditions (Ussiri and Lal, 2013; Butterbach-
506 Bahl et al., 2013; Suk, 2013; Oertel et al., 2016). Apart from reactive N availability, the main driver
507 of the aforementioned processes is soil moisture content (Butterbach-Bahl et al., 2013; Oertel et
508 al., 2016), and as the conditions change the N_2O production processes can switch rapidly between
509 the nitrification and the denitrification pathways (Skiba and Smith, 2000; Suk, 2013). The highest
510 N_2O efflux was observed in the control area (Fig. 7), where the soil moisture content, which is
511 considered to be the main driver for controlling N_2O emission (Megonigal et al., 2004; Oertel et al.,
512 2016), was the highest (54.87 %). We believe that the soil moisture content of the control area
513 was high enough to support denitrification, but still low enough for the nitrification processes to
514 occur, which could explain the highest emission values from this area. Shortly after the fire the flux
515 of N_2O started to decrease, and was significantly lower in the area burned in 1990. The soil
516 moisture can be the limiting factor for denitrification in the more recently burned areas, which
517 leads to the lower N_2O emissions measured there. Another reason for lower N_2O fluxes can be the
518 charcoal left on the forest floor after a forest fire (Kim, 2013; Oertel et al., 2016). It has been
519 observed that biochar amendment decreases N_2O emissions (Van Zwieten et al., 2015). This

finding can be applied to our work, as during the forest fire rather large amounts of charcoal were left on the forest floor and its action will still be similar to biochar, which ephemerally modifies the physical, chemical and biological properties of the soil (Van Zwieten et al., 2015). Earlier studies have reported lower N_2O emissions following the forest fires (Kim and Tanaka, 2003; Takakai et al., 2008). We noted that at more than 40 years after the forest fire the flux of N_2O increased and almost reached the pre-burning level (Fig. 7). Another aspect that can explain the N_2O emissions from our fire chronocequence areas is the ground vegetation composition. Soils are not the only sources that affect N_2O emissions. Cryptogams (lichens, bryophytes, etc.) can be a quite large sources for N_2O emissions (Lenhart et al., 2015). We also measured the emissions from the plants as the vegetation was not removed from the collar when the chamber was placed on top of it for the GHG measurements. Thus, the reasons why the N_2O emissions were higher in the control area compared to other areas can also be because there were more lichens and mosses that were emitting more N_2O.

We observed that forest fire had a substantial effect on all of the three measured GHGs and the effects were lasting for several decades after fire. There are numerous studies that deal with changes in GHG fluxes after fire disturbances (Burke et al., 1997; Sullivan et al., 2011; Köster et al., 2015), but only a few of them have studied the long term post-fire development of GHG fluxes on permafrost areas (Kim and Tanaka, 2003; Takakai et al., 2008). In addition to short-term effects, the impact of forest fires on soil GHG fluxes should be studied over decadal time scales due to the long lasting effects of forest fire on soil processes.

5. Conclusions

542 The long-term effects of fire on the fluxes of three main GHGs (CO_2, CH_4 and N_2O) in boreal
543 coniferous forest areas with underlying permafrost were investigated in this study. We used
544 existing knowledge to hypothesize that fire has an important influence on the fluxes of CO_2, CH_4
545 and N_2O, and the elapsed time since the last fire is the main factor that drives changes in fluxes of
546 these three GHGs. Our mixed model analysis revealed that the only factor that influenced all
547 measured GHGs was the time passed from last the forest fire. We also found that the impacts of a
548 forest fire on GHGs of our studied areas lasted for a rather long period of time. Soil CO_2 efflux
549 decreased after the fire, but increased thereafter for several decades and appeared to reach its
550 peak about 40–4 5 years later. Subarctic boreal forests acted as sinks of CH_4 in our study, but
551 changes in CH_4 fluxes lasted for a shorter period of time as the uptake of CH_4 did not differ
552 between the area burned in 1969 and the control area. Increases in active layer depth, in our
553 areas, did not lead to large increases in CH_4 fluxes. We also found that soil CH_4 uptake was
554 affected by soil temperature. A slight decrease in N_2O emission was observed in the comparison of
555 different fire age classes, and factors that appeared to influence fluxes of N_2O were C and N
556 contents of the soil, and also the depth of the active layer.

557

558 Acknowledgements

559 This study was supported by the Academy of Finland (Projects No. 286685, 294600, 307222) and
560 by ICOS Finland. We thank Saara Berninger for her help during the fieldwork. We also
561 acknowledge Alisdair Mclean (Language Center, University of Helsinki) for linguistic revision of this
562 paper, and for his valuable comments on the manuscript.

563

564 References

565 Amiro, B.D., Cantin, A., Flannigan, M.D., de Groot, W.J., 2009. Future emissions from Canadian
566 boreal forest fires. Can. J. Forest Res., 39, 383–395.

567 Anderson, D.M., Mauk, E.M., Wahl, E.R., Morrill, C., Wagner, A.J., Easterling, D., Rutishauser, T.,
568 2013. Global warming an independent record of the past 130 years. Geophys. Res. Lett., 40(1),
569 189–193.

570 Auclair, A.N.D., Carter, T.B., 1993. Forest wildfires as a recent source of CO_2 at northern latitudes.
571 Can. J. Forest Res., 23, 1528–1536.

572 Bates, D., Maechler, M., Bolker, B., Walker, S., 2015. Fitting Linear Mixed-Effects Models Using
573 lme4. Journal of Statistical Software, 67(1), 1–48. doi:10.18637/jss.v067.i01.

574 van Bellen, S., Garneau, M., Bergeron, Y., 2010. Impact of climate change on forest fire severity
575 and consequences for carbon stocks in boreal forest stands of Quebec, Canada: a synthesis. Fire
576 Ecology, 6(3), 16–44.

577 Brown, R.J.E., 1983. Effects of fire on permafrost ground thermal regime, in: Wein, R.W., MacLean,
578 D.A. (Eds.), The role of Fire in Northern Circumpolar Ecosystems. John Wiley, New York, pp. 97–
579 110.

580 Burke, R.A., Zepp, R.G., Tarr, M.A., Miller, W.L., Stocks, B.J., 1997. Effect of fire on soil-atmosphere
581 exchange of methane and carbon dioxide in Canadian boreal forest sites. J. Geophys. Res.,
582 102(D24), 29287–28300.

583 Burn, C.R., 1998. The response (1958-1997) of permafrost and near-surface ground temperatures
584 to forest fire, Takhini River valley, southern Yukon Territory. Can. J. Earth Sci., 35, 184–199.

585 Grubbs, F.E., 1969. Procedures for detecting outlying observations in samples. Technometrics, 11:
586 1–21.

587 Butterbach-Bahl, K., Baggs, E.M., Dannenmann, M., Kiese, R., Zechmeister-Boltenstern, S., 2013.
588 Nitrous oxide emissions from soils: how well do we understand the processes and their controls?
589 Philos. T. Roy. Soc. B, 368, 20130122. Http://dx.doi.org/10.1098/rstb.2013.0122

590 Cairney, J.W.G., Bastias, B.A., 2007. Influences of fire on forest soil fungal communities. Can. J. For.
591 Res. 37, 207–215. doi: 10.1139/X06-190.

592 Castaldi, S., Fierro, A., 2005. Soil-atmosphere methane exchange in undisturbed and burned
593 Mediterranean shrubland of Southern Italy. Ecosystems, 8(2), 182–190. doi:10.1007/s10021-004-
594 0093-z.

595 Chambers, J.M., 1992. Linear models. Chapter 4 of Statistical Models in S. In: Chambers, J.M. and
596 Hastie, T.J. (Eds.), Wadsworth & Brooks/Cole.

597 Conard, S.G., Sukhinin, A.I., Stocks, B.J., Cahoon, D.R., Davidenko, E.P., Ivanova, G.A., 2002.
598 Determining effects of area burned and fire severity on carbon cycling and emissions in Siberia.
599 Climatic Change 55: 197–211.

600 Dyrness, C.T., 1982. Control of depth to permafrost and soil temperature by the forest floor in
601 black spruce/feathermoss communities, USDA For. Serv. Pac. Northwest For. and Range Exp. Stn.,
602 Res. Note PNW-396, p. 19.

603 Dyrness, C.T., Norum, R.A., 1983. The effects of experimental fires on black spruce forest floors in
604 interior Alaska. Can. J. Forest Res., 13, 879–893.

605 Dore, S., Kolb, T.E., Montes-Helu, M., Sullivan, B.W., Winslow, W.D., Hart, S.C., Kaye, J.P., Koch,
606 G.W., Hungate, B.A., 2008. Long-term impact of a stand replacing fire on ecosystem CO_2 exchange
607 of a ponderosa pine forest. Glob. Change Biol. 14, 1801–1820.

608 Environment Canada, 2009. Canadian Climate Normals or Averages 1971–2000.
609 http://climate.weatheroffice ec.gc.ca/climate_normals/index_e.html (Accessed in April 2017]).

610 Fan, S., Gloor, M, Mahlman, J., Pacala, S., Sarmiento, J., Takashi, T., Peng, T., 1998. A large
611 terrestrial carbon sink in North America implied by atmospheric and oceanic carbon dioxide data
612 and models. Science, 282, 442–446.

613 Faraway, J.J., 2002. Practical Regression and Anova using R. In: Reproduction. pp. 88–91.

614 Fiedler, S., Höll, B.S., Jungkunst, H.F., 2005. Methane budget of a Black Forest spruce ecosystem
615 considering soil pattern. Biogeochemistry, 76(1), 1–20.

616 Flannigan, M.D., Stocks, B.J., Wotton, B.M., 2000. Climate change and forest fires. Sci. Total
617 Environ., 262, 221–229.

618 Gewehr, S., Drobyshev, I., Berninger, F., Bergeron, Y., 2014. Soil characteristics mediate the
619 distribution and response of boreal trees to climatic variability. Can. J. For. Res., 44(5), 487–498,
620 10.1139/cjfr-2013-0481.

621 Gill, H.K., Lantz, T.C., O'Neill, B., Kokelj, S.V., 2014. Cumulative Impacts and Feedbacks of a Gravel
622 Road on Shrub Tundra Ecosystems in the Peel Plateau, Northwest Territories, Canada. Arct.
623 Antarct. Alp. Res., 46, 947-961.

624 Grosse, G., Harden, J., Turetsky, M., McGuire, A.D., Camill, P., Tarnocai, C., Frolking, S., Schuur,
625 E.A.G., Jorgenson, T., Marchenko, S., Romanovsky, V., Wickland, K.P., French, N., Waldrop, M.,

626 Bourgeau-Chavez, L., Striegl, R.G., 2011. Vulnerability of high-latitude soil organic carbon in North
627 America to disturbance. Journal of Geophysical Research: Biogeosciences, 116, G00K06.

628 Hadlari, T., 2006. Sedimentology of Cretaceous Wave-Dominated Parasequences, Trevor
629 Formation, Peel Plateau, NWT. Yellowknife: Northwest Territories Geosciences Office, 16 pp.

630 Hamman, S.T., Burke, I.C., Stromberger, M.E., 2007. Relationships between microbial community
631 structure and soil environmental conditions in a recently burned system. Soil Biol. Biochem., 39,
632 1703–1711. doi: 101016/j.soilbio.2007.01.018.

633 Hanson, R.S., Hanson, T.E., 1996. Methanotrophic bacteria. Microbiol. Mol. Biol. R., 60, 439–471.

634 Hart, S.C., DeLuca, T.H., Newman, G.S., MacKenzie, M.D., Boyle, S.I., 2005. Post-fire vegetative
635 dynamics as drivers of microbial community structure and function in forest soils. For. Ecol.
636 Manage., 220, 166–184.

637 Hinzman, L.D., Kane, D.L., Gieck, R.E., Everett, K.R., 1991. Hydrologic and thermal properties of the
638 active layer in the Alaskan Arctic. Cold Reg. Sci. Technol., 19, 95–110.

639 Houghton, R.A., House, J.I., Pongratz, J., van der Werf, G.R., DeFries, R.S., Hansen, M.C., Le Quére,
640 C., Ramankutty, N., 2012. Biosciences, 9, 5125–5142.

641 IFFN – International Forest Fire News, 2004. No.31 (July-December), 122–131. Available from:
642 http://www.fire.uni-freiburg.de/iffn/iffn_31/19-IFFN-31-Boreal-Climate-2.pdf (Accessed in
643 December 2016)

644 IUSS Working Group WRB. 2015. World Reference Base for Soil Resources 2014, update 2015

645 International soil classification system for naming soils and creating legends for soil maps.

World Soil Resources Reports No. 106. FAO, Rome.

Kasischke, E.S., Christensen, N.L., Jr., Stocks, B.J., 1995. Fire, global warming, and the carbon balance of boreal forests. Ecol. Appl., 5(2), 437–451.

Kasishcke, E.S., Stocks, J.B. (Eds.), 2000. Fire, Climate Change, and Carbon Cycling in the Boreal Forest, Ecological Studies 138, Springer-Verlag, New York, 461 pp.

Kasurinen, V., Alfredsen, K., Kolari, P., Mammarella, I., Alekseychik, P., Rinne, J., Vesala, T., Bernier, P., Boike, J., Langer, M., Marchesini, L.B., Van Huissteden, K., Dolman, H., Sachs, T., Ohta, T., Varlagin, A., Rocha, A., Arain, A., Oechel, W., Lund, M., Grelle. A., Lindroth, A., Black A., Aurela, M., Laurila, T., Lohila, A., Berninger, F., 2014. Latent heat exchange in the boreal and arctic biomes. Glob. Change Biol., 20, 3439–3454, doi: 10.1111/gcb.12640.

Kätterer, T., Reichstein, M., Andrén, O., Lomander, A., 1998. Temperature dependence of organic matter decomposition: a critical review using literature data analyzed with different models. Biol. Fert. Soils, 27(3), 258–262.

Kim, Y.S., 2013. Soil-atmosphere exchange of CO_2, CH_4 and N_2O in northern temperate forests: effects of elevated CO_2 concentration, N deposition and forest fire. Eurasian Journal of Forest Research 16(1), 1–43.

Kim, Y., Tanaka, N., 2003. Effect of forest fire on the fluxes of CO_2, CH_4 and N_2O in boreal forest soils, interion Alaska. J. Geoph. Res., 108, NO.D1, 8154, FFR 10-1 – FRR 10-11. doi: 10.1029/2001JD000663.

Kimble, J.M., 2004. Cryosols: Permafrost-Affected Soils. Springer, Germany, 726 pp.

666 Klock, G.O., Helvey, J.D., 1976. Soil-water trends following wildfire on the Entiat, Experimental
667 Forest. Annual Proceedings Tall Timbers Fire Ecologic Conference, 15, 193–200.

668 Knicker, H., 2007. How does fire affect the nature and stability of soil organic nitrogen and carbon?
669 A review. Biogeochemistry 85, 91–118.

670 Köster, E., Köster, K., Berninger, F., Pumpanen, J., 2015. Carbon dioxide, methane and nitrous
671 oxide fluxes from podzols of a fire chronosequence in the boreal forests in Värriö, Finnish Lapland.
672 Geoderma Regional, 5, 181–187.

673 Köster, K., Berninger, F., Lindén, A., Köster, E., Pumpanen, J., 2014. Recovery in fungal biomass is
674 related to decrease in soil organic matter turnover time in a boreal fire chronosequence.
675 Geoderma, 235–236, 74–82.

676 Köster K., Berninger F., Heinonsalo J., Lindén A., Köster E., Ilvesniemi H., Pumpanen J., 2016. The
677 long-term impact of low-intensity surface fires on litter decomposition and enzyme activities in
678 boreal coniferous forests. Int. J. Wildland Fire, 25(2), 213–223.

679 Kulmala L., Aaltonen H., Berninger F., Kieloaho A.-J., Levula J., Bäck J., Kolari P., Korhonen J.F.J.,
680 Nikinmaa E., Pihlatie M., Vesala T., Pumpanen J., 2014. Changes in biogeochemistry and carbon
681 fluxes in a boreal forest after a clear cut and partial burning of slash. Agr. Forest Meteorol., 188,
682 33–44.

683 Kurz, W.A., Apps, M.J., 1999. A 70-year retrospective analysis of carbon fluxes in the Canadian
684 forest sector. Ecol. Appl., 9(2), 526–547.

685 Lambert, M.C., Ung, C.H., Raulier, F., 2005. Canadian national tree aboveground biomass
686 equations. Can. J. For. Res., 35, 1996–2018.

687 Lenhart, K., Weber, B., Elbert, W., Steinkamp, J., Clough, T., Crutzen, P., Pöschl, U., Keppler, F.,
688 2015. Nitrous oxide and methane emissions from cryptogamic covers. Glob. Change Biol., 21,
689 3889–3900.

690 Levine, J.S., Cofer, W.R., Sebacher, D.I., Winstead, E.L., Secacher, S., Boston, P.J., 1988. The effects
691 of fire on biogenetic soil emissions of nitric oxide and nitrous oxide. Global Biogeochemistry
692 Cycles, 2, 445–449.

693 Liang, L.-H., Zhou, Y.-W., Wang, J.C., 1991. Changes to the permafrost environment after forest
694 fire, Da Xi'an Ridge, Gu Lian Mining Area, China. Permafrost Periglac., 2, 253–257.

695 Lyons, E.A., Jin, Y., Randerson, J.T., 2008. Changes in surface albedo after fire in boreal forest
696 ecosystems of interior Alaska assessed using MODIS satellite observations. J. Geophys. Res., 113,
697 G02012, doi: 10.1029/2007JG000606.

698 Megonigal, J.P., Hines, M.E., Visscher, P.T., 2004. Anaerobic Metabolism: Linkages to Trace Gases
699 and Aerobic Processes, in: Schelesinger, W.H. (Ed.) Biogeochemistry. Elsevier-Pergamon, Oxford,
700 UK. pp. 317–424.

701 Meikle, J. C., Waterreus, M. B., 2008: Ecosystems of the Peel River watershed: A predictive
702 approach to regional ecosystem mapping. Whitehorse: Fish and Wildlife Branch, Department of
703 Environment, Government of Yukon, 66 pp.

704 Nakano, T., 2006. Changes in surface methane flux after a forest fire in West Siberia, in: Hatano,
705 R., Guggenberger, G. (Eds.), Symptom of Environmental Change in Siberian Permafrost Region.
706 Hokkaido University Press, Sapporo, pp. 55–63.

707 Oertel, C., Matschullat, J., Zurba, K., Zimmermann, F., Erasmi, S., 2016. Greenhouse gas emissions
708 from soils – A review. Chem. Erde, 76(3), 327–352.

709 Pereira, P., Cerdá, A., Bolutiene, V., Úbeda, X., Pranskevicius, M., Jordán, A., Zavala, L.M., Mataiz-
710 Solera, J. 2013. Spatio-temporal effects of low severity grassland fire on soil colour. Geophysical
711 Research Abstracts 15, EGU2013-10641.

712 Pihlatie, M., Pumpanen, J., Rinne, J., Ilvesniemi, H., Simojoki, A., Hari, P., Vesala, T., 2007. Gas
713 concentrations driven fluxes of nitrous oxide and carbon dioxide in boreal soil. Tellus 59B, 458–
714 469. doi: 10.1111/j.1600-0889.2007.00278.x.

715 Pihlatie, M., Christiansen, J.R., Aaltonen, H., Korhonen, J.F.J., Nordbo, A., Rasilo, T., Benanti, G.,
716 Giebels, M., Helmy, M., Sheehy, J., Jones. S., Juszczak, R., Klefoth, R., Lobo-do-Vale, R., Rosa, A.P.,
717 Schreiber, P., Serca¸ D., Vicca, S., Wolf, B., Pumpanen, J., 2013. Comparison of static chambers to
718 measure CH_4 emissions from soils. Agr. Forest Meteorol., 171–172, 124– 136.
719 http://dx.doi.org/10.1016/j.agrformet.2012.11.008

720 Poth, M., Anderson, I.C., Miranda, H.S., Miranda, A.C., Riggan, P.J., 1995. The magnitude and
721 persistence of soil NO, N_2O, CH_4 and CO_2 fluxes from burned tropical savanna in Brasil. Global
722 Biochem. Cy., 9(4), 503–513.

723 Pumpanen, J., Kolari, P., Ilvesniemi, H., Minkkinen, K., Vesala, T., Niinisto, S., Lohila, A., Larmola, T.,
724 Morero, M., Pihlatie, M., Janssens, I., Yuste, J.C., Grunzweig, J.M., Reth, S., Subke, J.A., Savage, K.,
725 Kutsch, W., Ostreng, G., Ziegler, W., Anthoni, P., Lindreth, A., Hari, P., 2004. Comparison of
726 different chamber techniques for measuring soil CO2 efflux. Agr. Forest Meteorol., 123, 159–176.

727 Rayment, M.B., Jarvis P.G., 2000. Temporal and spatial variation of soil CO_2 efflux in a Canadian
728 boreal forest. Soil Biol. Biochem., 32, 35–45.

729 Richter, D.D., O'Neill, K.P., Kasischke, E.S., 2000. Postfire stimulations of microbial decomposition
730 in black spruce (Picea marinara L.) forest soils, in: Kasischke E.S., Stocks, B.J., (Eds.), A Hypothesis,

731 in Fire, Climate Change, and Carbon Cycling in the Boreal Forest. Springer-Verlag, New York, pp.
732 197–213.

733 Saiz, G., Byrne, K.A., Butterbach-Bahl, K., Kiese, R., Blujdea, V., Farrell, E.P., 2006. Stand age-related
734 effects on soil respiration in a first rotation Sitka spruce chronosequence in central Ireland. Glob.
735 Change Biol., 12, 1007–1020.

736 Sharrow, S.H. and Wright, H.A., 1977. Effects of fire, ash and litter on soil nitrate, temperature,
737 moisture and tobosagrass production in the Rolling Plains. Journal of Range Management, 30(4),
738 266-270.

739 Sirois, L., 1993. Impact of fire on Picea mariana and Pinus banksiana seedlings in subarctic lichen
740 woodlands. J. Veg. Sci., 4(6), 795–802.

741 Skiba, U., Smith, K.A., 2000. The control of nitrous oxide emissions from agricultural and natural
742 soils. Chemosphere – Glob. Change Sci., 2, 379–386.

743 Stanek, W., 1982. Reconnaissance of vegetation and soils along the Dempster Highway, Yukon
744 Territory: II. Soil properties as related to revegetation. In, Pacific Forest Research Centre. Canadian
745 Forestry Service; no. BC-X-236. Canadian Forestry Service, Victoria, 34 p.

746 Stefansky, W., 1972. Rejecting Outliers in Factorial Designs. Technometrics, 14, 469–479.

747 Stocks, B.J., Fosberg, M.A., Lynham, T.J., Mearns, L., Wotton, B.M., Yang, Q., Jin, J-Z., Lawrence, K.,
748 Hartley, G.R., Mason, J.A., McKenney, D.W., 1998. Climate Change and Forest Fire Potential in
749 Russian and Canadian Boreal Forests. Climatic Change, 38, 1–13.

750 Suk, K.J., 2013. Soil-Atmosphere Exchange of CO2, CH4 and N2O in Northern Temperate Forests:
751 Effects of Elevated CO2 Concentration, N Deposition and Forest Fire. Eurasian Journal of Forest
752 Research, 16(1), 1–43.

753 Sullivan, B.W., Kolb, T.E., Hart, S.C., Kaye, J.P., Hungate, B.A., Dore, S., Montes-Helu, M., 2011.
754 Wildfire reduces carbon dioxide efflux and increases methane uptake in ponderosa pine forest
755 soils of southwestern USA. Biogeochemistry, 104, 251–265. doi: 10.1007/s10533-010-9499-1.

756 Takakai, F., Desyatkin, R., Lopez, C.M.L., Fedorov, A.N., Desyatkin, R.V., Hatano, R., 2008. Influence
757 of forest disturbance on CO_2, CH_4 and N_2O fluxes from larch forest soil in the permafrost taiga
758 region of eastern Siberia. Soil Sci. Plant Nutr., 54, 938–949.

759 Taş, N., Prestat, E., McFarland, J.W., Wickland, K.P., Knight, R., Berhe, A.A., Jorgenson, T., Waldrop,
760 M.P., Jansson, J.K., 2014. Impact of fire on active layer and permafrost microbial communities and
761 metagenomes in an upland Alaskan boreal forest. The ISME Journal, 8:1904-1919. doi:
762 10.1038/ismej.2014.36.

763 Tsuyuzaki, S., Kushida, K., Kodama, Y., 2008. Recovery of surface albedo and plant cover after
764 wildfire in a Picea mariana forest in interior Alaska. Climatic Change, 93, 517.

765 Ullah, S., Moore, T.R., 2011. Biochemical controls on methane, nitrous oxide, and carbon dioxide
766 fluxes from deciduous forest soils in eastern Canada. J. Geophys. Res., 116, G03010.

767 Ussiri, D., Lal, R., 2013. Soil Emissions of Nitrous Oxide and Its Mitigation. Springer, Dordrecht, pp.
768 378.

769 Van Zwieten, L., Kammann, C., Cayuela, M.L., Singh, B.P., Joseph, S., Kimber, S., Donne, S., Clough,
770 T., Spokas, K.A., 2015. Biochar effects on nitrous oxide and methane emissions from soil, in:

771 Lehmann J., Joseph, S., (Eds.): Biochar for Environmental management – Science, Technology and
772 Implementation. 2nd Ed. Routledge Taylor & Francis Group, London & New York, pp. 489–520.

773 Viereck, L.A., 1982. Effects of fire and firelines on active layer thickness and soil temperatures in
774 interior Alaska, in Proceedings of the 4th Canadian Permafrost Conference, The Roger J.E. Brown
775 Memorial Volume, pp. 123–134. Natl. Res. Counc. Of Can., Ottawa, Ontario, Canada.

776 Viereck, L.A., 1983. The effects of fire in black spruce ecosystems of Alaska and northern Canada,
777 in Wein R.W., MacLean, D.A. (Eds.): The role of fire in northern circumpolar ecosystems (Scope
778 18). John Wiley and Sons, Chishester, England, pp. 201–220.

779 Wagner, R.G., Ter-Mikaelian, M.T., 1999. Comparison of biomass component equations for four
780 species of northern coniferous tree seedlings. Ann. For. Sci., Springer Verlag/EDP Sciences, 56(3),
781 193–199.

782 Wang, W., Wang, H., Zu, Y., Li, X., Koike, T., 2006. Characteristics of the temperature coefficient,
783 Q19, for the respiration of non-photosynthetic organs and soils of forest ecosystems. Front.
784 Forest. China, 1(2), 125–135.

785 Whalen, S.C., Reeburgh, W. S., Barber, V.A., 1992. Oxidation of methane in boreal forest soils: a
786 comparison of seven measures. Biogeochemistry, 16, 181–211.

787 Yoshikawa K., Bolton, W.R., Romanovsky, V.E., Fukuda, M., Hinzman, L.D., 2003. Impacts of
788 wildfire on the permafrost in the boreal forests of Interior Alaska. J. Geophys. Res., 107(8148),
789 FFR4-1–FFR4-14. doi:10.1029/2001JD000438.

790 Zavala, L.M., de Celis, R. Jordán, 2014. How wildfires affect soil properties. A brief rewiew.
791 Cuadernos de Investigación Geográfica. 40(2), 311-331.

792 Zona, D., 2016. Long-term effects of permafrost thaw. Nature, 537, 625–626.

Table1
Click here to download Table: Table 1.docx

Table 1. Mean soil temperatures (˚C), soil moisture (%), soil pH, soil C and N contents (%) (Control n=24, 1969 n=22, 1990 n=23, 2012 n=26; soil samples collected from depths of 0.05 m , 0.1 m, 0.3 m, 0.5 m and on top of the permafrost), depth of active layer (m), ground vegetation biomass (kg m^{-2}) and coverages (%), and living tree biomass (kg m^{-2})of the studied fire chronosequence areas. Letters besides the mean values mark the significant differences ($p < 0.05$) between the analyzed fire age classes. Correlation coefficients for fire age classes (n=68), statistical significance for measured variables ($P < 0.05$) is marked with *.

	Soil temperature at 10 cm depth (˚C)	Average soil moisture (%)	Soil pH	Soil C (%)	Soil N (%)	Depth of active layer (m)	Ground vegetation coverage (%) (vascular plants/moss + lichens)	Ground vegetation biomass (kg m^{-2}) (vascular plants/moss + lichens)	Living tree biomass (kg m^{-2})
Control	4.3^{A}	54.9^{A}	5.06^{AB}	28.4^{A}	0.9^{A}	0.28^{A}	$37.4^{A}/87.4^{A}$	$0.6^{A}/1.0^{A}$	5.24^{A}
1969	5.3^{B}	49.1^{AB}	6.73^{A}	16.5^{B}	0.8^{A}	0.49^{B}	$47.2^{A}/63.2^{B}$	$0.7^{A}/0.6^{B}$	3.50^{B}
1990	7.7^{A}	40.3^{BC}	5.16^{B}	15.5^{B}	0.5^{B}	0.88^{BC}	$33.4^{A}/66.1^{B}$	$0.7^{A}/0.7^{B}$	0.09^{C}
2012	6.8^{A}	37.2^{C}	4.18^{B}	10.8^{C}	0.5^{B}	1.01^{C}	$15.5^{B}/4.0^{C}$	$0.3^{C}/0.2^{C}$	0^{C}
Correlation coefficients	-0.503*	0.334*	-0.243*	0.583*	0.387*	-0.549*	0,354*	0.360*	0.703*

Table 2
Click here to download Table: Table 2.docx

Table 2. Linear mixed effect models fitted against CO2, CH4 and N2O fluxes and experimental factors. The fixed effects in the model were CO_2, CH_4, N_2O – greenhouse gas concentrations; YR – time since last fire (yrs.); ST – soil temperature at 0.10 m depth (°C) ; AD – active layer depth (m); TB – tree biomass (kg m^{-3}); GB – ground vegetation biomass (kg m^{-3}); r(YL) means the random effect (collars in sample line) and ε the error term. The models in bold are the best fitted model.

CO_2	Mixed effect model Equations	r^2	*P*	Intercept	AIC	df
Model 1	$CO_2 = a + b$YR + cST + dMOI + eAD + fTB + gGB + h(ST x AD) + *r(YL)*	0,51	0,0045	0,483	-80,913	12
Model 2	$CO_2 = a + b$YR + cST + dAD + eTB + fGB + g(ST x AD) + *r(YL)*	0,50	0,0024	0,451	-82,907	11
Model 3	$CO_2 = a + b$YR + cST + dAD + eTB + f(ST x AD) + *r(YL)*	0,49	0,0012	0,429	-84,835	10
Model 4	$CO_2 = a + b$YR + cST + dAD + f(ST x AD) + *r(YL)*	0,49	0,0006	0,406	-86,666	9
Model 5	$CO_2 = a + b$YR + cST + dAD + *r(YL)*	0,50	0,0003	0,442	-88,506	8
Model 6	$CO_2 = a + b$YR + cST + *r(YL)*	0,50	0,0001	0,436	-90,439	7
Model 7	**$CO_2 = a + b$YR + *r(YL)***	**0,50**	**3,69E-05**	**0,455**	**-92,226**	**6**
CH_4						
Model 1	$CH_4 = a + b$YR + cST + dMOI + eAD + fTB + egGB + h(ST x AD) + *r(YL)*	0,32	0,0265	-2,08E-05	-1402,6	12
Model 2	**$CH_4 = a + b$YR + cST + dMOI + eAD + fTB+ g(ST x AD) + *r(YL)***	**0,33**	**0,0158**	**-1,63E-05**	**-1405**	**10**
N_2O						
Model 1	$N_2O = a + b$YR+ cST + dMOI + eAD + fTB+ gGB + h(ST x AD) + *r(YL)*	0,30	0,0015	2,47E-06	-1666,9	12
Model 2	**$N_2O = a + b$YR + cST + dMOI + eAD + fTB + g(ST x AD) + *r(YL)***	**0,30**	**0,00086**	**2,65E-06**	**-1668,6**	**11**

Figure1
Click here to download Figure: Figure1.docx

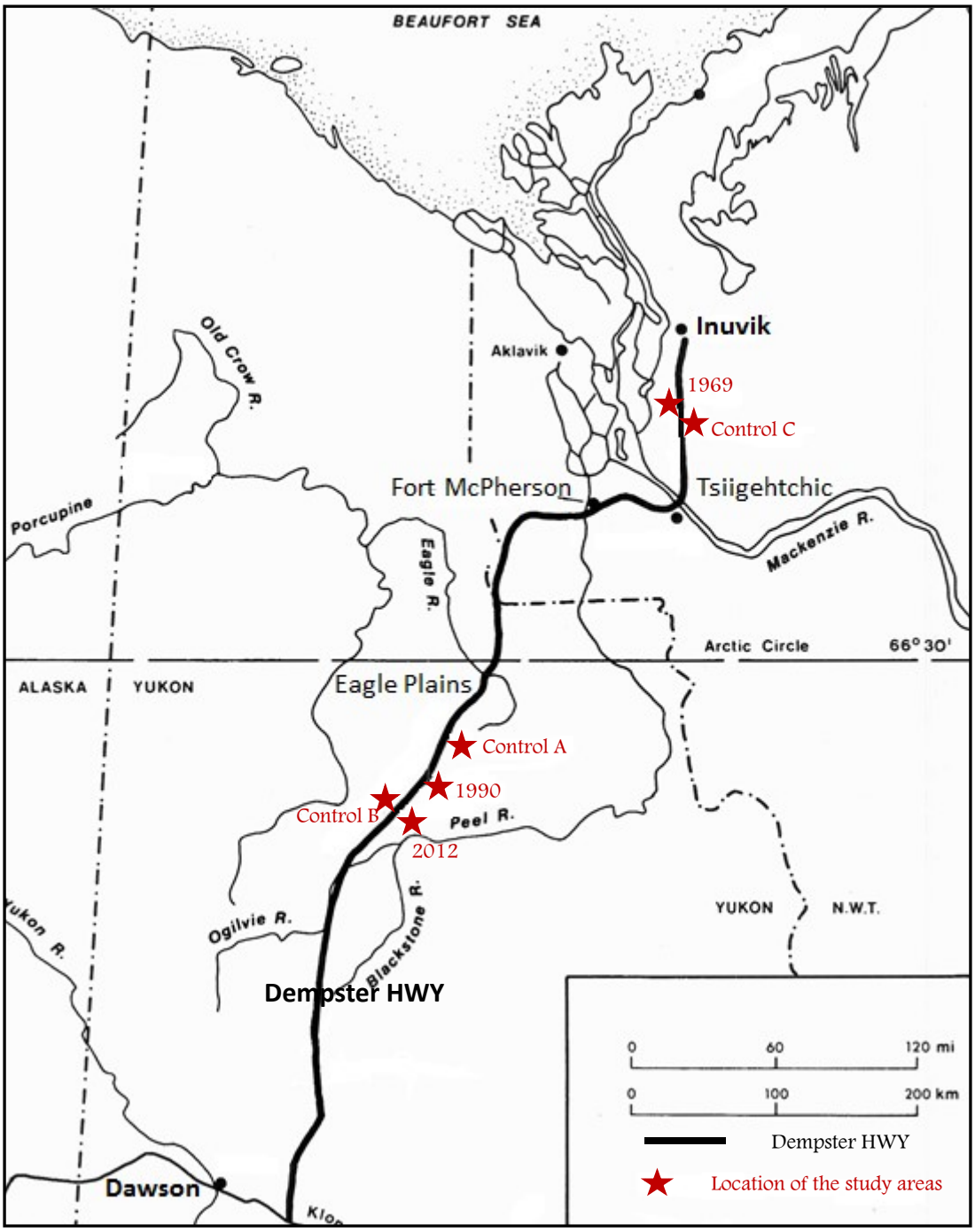

Figure 1. Location of the study areas along the Dempster Highway, Yukon and Northwest Territories, Canada.

Figure2
Click here to download Figure: Figure2.docx

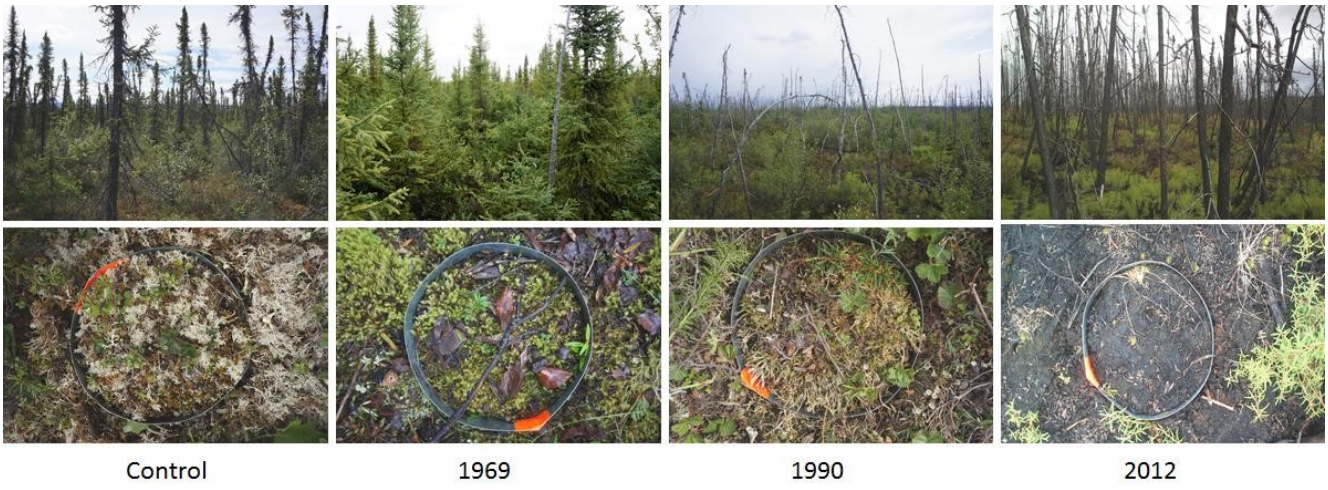

Figure 2. Appearance of different study areas along the Dempster Highway, Yukon and Northwest Territories, Canada (stand level and ground vegetation level).

Figure3
Click here to download Figure: Figure3.docx

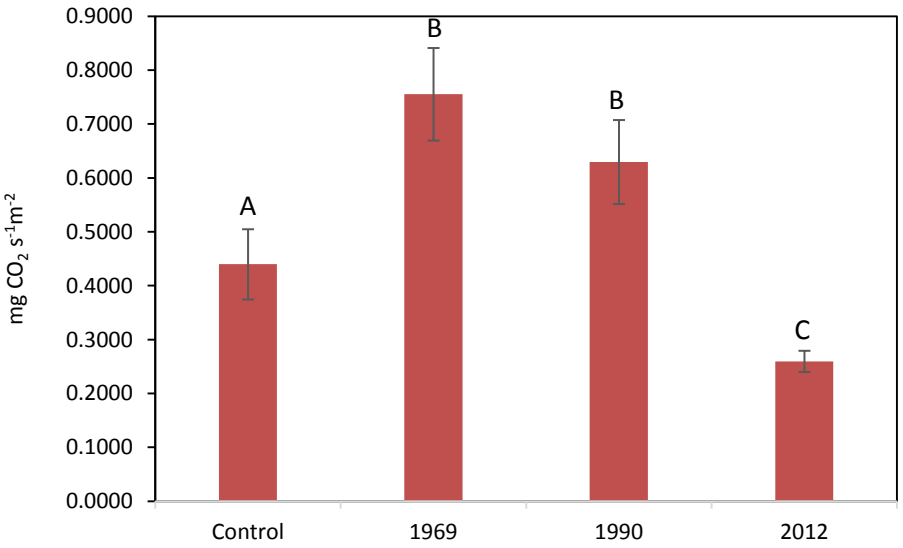

Figure 2. Averages of temperature corrected carbon dioxide (CO_2) fluxes during the summer of 2015 (n = 58 per measurement period). Hanging bars represent the analyzed fire age classes (date of forest fire marked under the bars). Vertical bars represent standard errors. Letters above the bars indicate the statistically significant difference ($P < 0.05$).

Figure4

Click here to download Figure: Figure4.docx

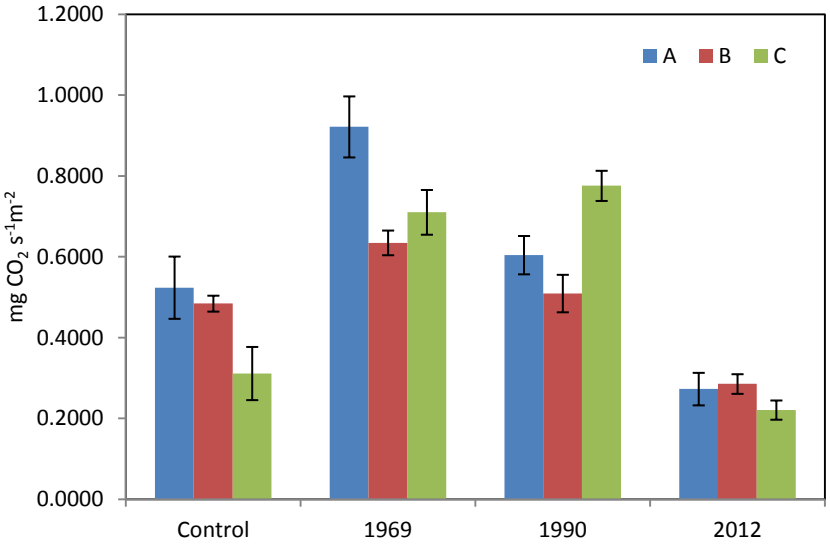

Figure 3. Average fluxes of temperature corrected carbon dioxide (CO_2) during summer 2015 on three lines (marked as A, B, C) per fire age class (date of forest fire marked under the columns) (n = 18 per site). Vertical bars represent standard errors.

Figure5
Click here to download Figure: Figure5.docx

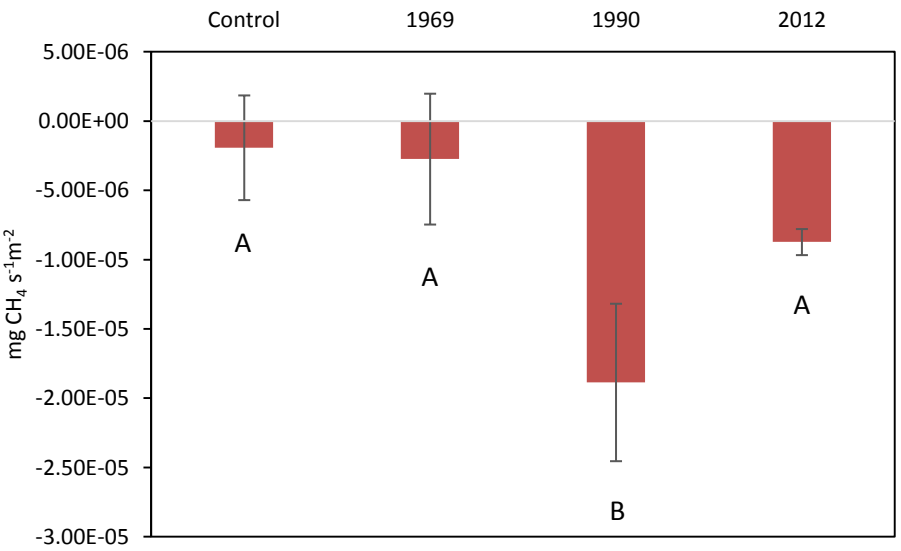

Figure 4. Average fluxes of methane (CH_4) during summer 2015 (n = 59 per measurement period). Hanging bars represent the analyzed fire age classes (date of forest fire marked under the bars). Vertical bars represent standard errors. Letters below the data points indicate the statistically significant difference ($P < 0.05$).

Figure6
Click here to download Figure: Figure6.docx

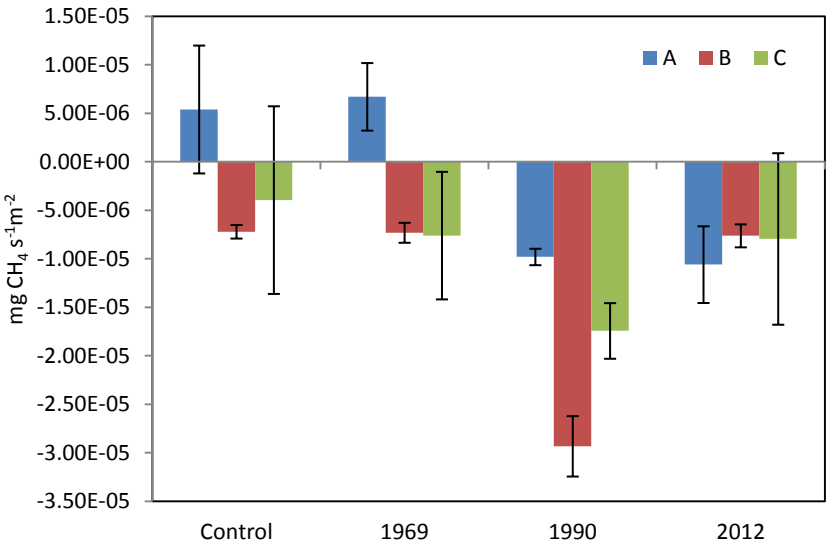

Figure 5. Average fluxes of methane (CH_4) during summer 2015 on three lines (marked as A, B, C) per fire age class (date of forest fire marked under the columns) (n = 16 per site). Vertical bars represent standard errors.

Figure7
Click here to download Figure: Figure7.docx

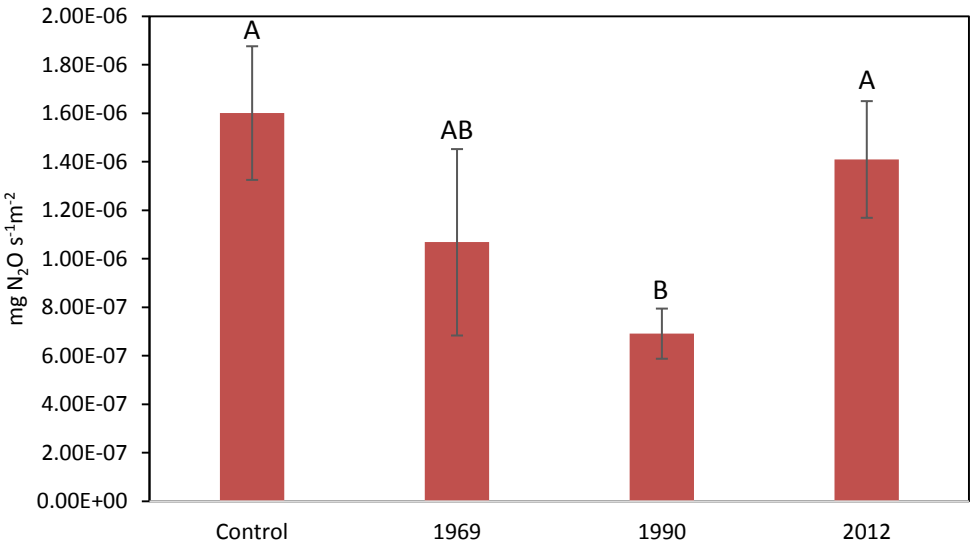

Figure 6. Average N_2O fluxes measured in the summer of 2015 (n = 46 per measurement period). Hanging bars represent the analyzed fire age classes (date of forest fire marked above the bars). Vertical bars represent standard errors. Letters below the data points indicate the statistically significant difference ($P < 0.05$).

Figure8
Click here to download Figure: Figure8.docx

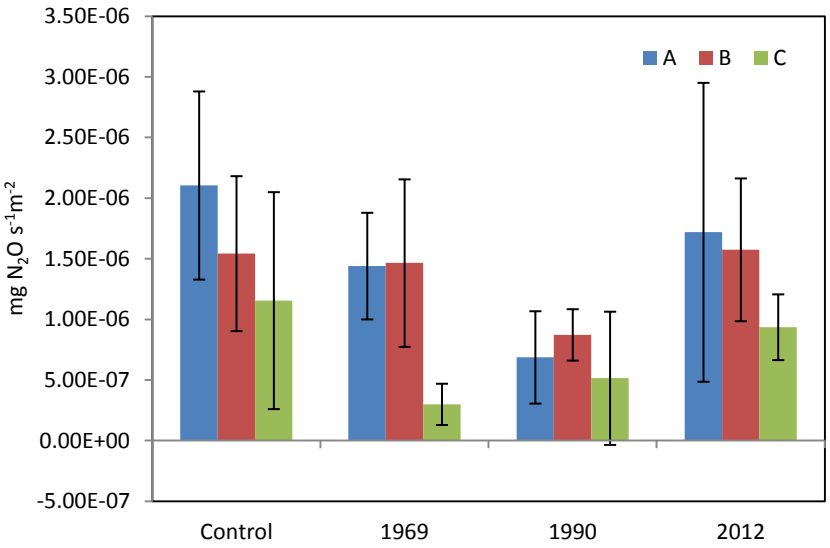

Figure 7. Average fluxes of nitrous oxide (N_2O) during summer 2015 on three lines (marked as A, B, C) per fire age class (date of forest fire marked under the columns) (n = 16 per site). Vertical bars represent standard errors.